

# Time characteristics for the spinodal decomposition in nuclear matter

D. Idier, M. Farine, B. Benhassine, B. Remaud and F. Sebillé

Laboratoire de Physique de Nucléaire, CNRS/IN2P3, Université de Nantes

2, rue de la Houssinière F 44072 NANTES CEDEX 03

**ABSTRACT :** Dynamical instabilities arising from fluctuations in spinodal zone for nuclear matter are studied using Skyrme type interactions within a pseudo-particle model. Typical times for cluster formation are extracted.

PACS numbers : 05.70.Ln, 21.65+f, 64-60-i

The phase space diagram of infinite nuclear matter possesses zones of mechanical instabilities, where the initially homogeneous system is unstable against the growth of density fluctuations and may separate into two phases : liquid drops surrounded by vapor or bubbles inside a liquid phase, depending on the average density of the system. Such a transition could be at the origin of the increase in the yield of intermediate fragments observed in heavy ion reactions above 30 MeV/u.

The growth of density fluctuations in infinite Fermi fluids has been analytically treated [1] and applied to the nuclear fragmentation [2]; this theory is based on a generalization of Landau's kinetic equation and allows the qualitative classification of the behaviours expected in heavy ion reactions according to the initial conditions in the  $(T, n)$  plane. Such an analytical approach however is strictly limited to the linear regime, it provides the domain of critical initial conditions but not the non-linear development of the instabilities. Furthermore, Landau's equation is based on the concept of quasi-particles which is meaningful for small excitation of real particles close to the Fermi level, which is far from being the situation in real heavy ion collisions.

In another context, using canonical Metropolis simulations, Peilert et al. [3] were able to show that clusters develop at subsaturation energy in nuclear matter. In a dynamical context D. Boal et al. [4] using a quasiparticle model with a simplified interaction have shown (for small time) that the growth of fluctuations is exponential with a time constant of 25 fm/c.

This paper aims at getting insight in the dynamics of the fluctuation growth; since in actual reactions such a process is in competition with many others (cooling by evaporation, sequential emissions...), time characteristics are then key quantities in order to determine the conditions under spinodal decomposition could be observed.

Our numerical treatment is based on the Vlasov phase space transport equation, complemented by a Pauli-blocked Uehling-Uhlenbeck collision term (see [5] for a review). This equation is usually solved using the projection of the phase space density distribution on a set of

pseudo-particles; we shall use the so-called Landau-Vlasov model [6] where the pseudo-particles are gaussians in space and momentum, their width and number choosen to reproduce the nucleus surface diffuseness and to optimize the uniformity of the phase space paving [7].

The pseudo-particles (PP) Hamiltonian in phase space reads :

$$H_{pp} = \frac{\langle \vec{p}^2 \rangle}{2m} + \langle V_{HF}(\vec{r}, \vec{p}) \rangle \quad (1)$$

where  $V_{HF}$  is the Wigner-transformed Hartree-Fock nuclear potential,  $m$  the nuclear mass. The brackets indicate that the above quantities are smeared out by the (here gaussian) form factor of the pseudo-particles; the solution of the Landau-Vlasov equation gives the time evolution of a swarm of pseudo-particles moving in the field of equation (1) and undergoing binary collisions when allowed by the phase space availability. The cross section of pseudo-particles is scaled on the nucleon-nucleon cross section such that their average mean free path is kept equal to the nucleon one [5,7].

We first report here on infinite matter calculations; its properties will be studied in a cubic box with periodic boundary conditions; the system is taken homogeneous in  $r$ -space with a Fermi-Dirac momentum distribution; its initial phase space distribution then reads :

$$f(\vec{r}, \vec{p}; t=0) = \frac{1}{n_g} \sum_{i=1}^N g_x(\vec{r} - \vec{r}_i) g_p(\vec{p} - \vec{p}_i) \quad (2)$$

and the spatial density  $n$  is :

$$n(\vec{r}; t=0) = \frac{1}{n_g} \sum_{i=1}^N g_x(\vec{r} - \vec{r}_i) \quad (3)$$

the  $g_\Delta$  - functions are normalized gaussians with a width  $\Delta$ ; the  $(r_i, p_i)$  coordinates of each gaussians are randomly drawn according to the probability density law  $d(\epsilon)$  :

$$\begin{aligned} d(\epsilon_i) &= \theta(\epsilon_F - \epsilon_i) & \text{for } T = 0 \\ d(\epsilon_i) &= [1 + \exp((\epsilon_i - \epsilon_F)/T)]^{-1} & \text{for } T \neq 0 \end{aligned} \quad (4)$$

The Fermi energy  $\epsilon_F$  is constrained on the initial nuclear density  $n_0$ ; the number  $N$  of pseudo-particles then follows as :

$$N = n_0 L^3 n_g \quad (5)$$

$L$  being the linear dimension of the cube and  $n_g$  the number of pseudo-particles associated with each nucleon.

We compare the nuclear Equation Of State (EOS) with the pseudo-particles model against the analytical one, in the case of a Skyrme Skm\* interaction [8] :

$$\begin{aligned} V_{HF}(\vec{r}) &= \frac{3}{4} t_0 n(\vec{r}) + \frac{1}{16} [3t_1 + (5 + 4\kappa_2)t_2] \int \frac{\vec{p}^2}{2m} f(\vec{r}, \vec{p}) d\vec{p} \\ &+ \frac{1}{32} [(5 + 4\kappa_2)t_2 - 9t_1] \Delta n(\vec{r}) + \frac{3}{8} t_3 (\gamma + 2) n(\vec{r})^{\gamma+1} \end{aligned} \quad (6)$$

Figure 1 shows that one can reproduce with a great precision the exact EOS (known from HF calculations), as soon as  $n_g$  is sufficiently large [7], ( $n_g > 40$ ). Note that for the whole range of temperatures and densities the gaussian widths  $\Delta$  of (2) are set constant. Detailed studies [7] show too that the Landau parameters  $F_0$  and  $F_1$  are reproduced at a sufficient level of accuracy, and then the above formalism provides a good approximation to the Landau kinetic theory in the linear regime. However, it presents the advantage of not being specialized to the small excitation regime, of including a microscopic treatment of binary collisions, and of being suitable for finite systems. The droplet (bubble) formation is a process where the surface properties or nucleon effective mass could play a decisive role, being easily treated since a larger variety of nuclear effective interactions can be implemented in the model.

In figure 2, we show two snapshots of a system initially prepared in the spinodal zone of instability ( $n=0.0492 \text{ fm}^{-3}$ ,  $T=3 \text{ MeV}$ ). To get a better view, several periodic boxes have been associated. At initial time, the pseudo-particles are randomly and uniformly scattered whereas at  $t=165 \text{ fm/c}$  strong inhomogeneities show up : large clusters of nuclear liquid embedded in a vapor phase. These structures are stable with time; they do not look like nuclei, in particular due to absence of Coulomb field which would help breaking them into small pieces. The box size  $L$  is  $16 \text{ fm}$ , sufficiently large to get independence of the results on the boundary conditions;  $L$  is a critical parameter, using a too small box would prevent inhomogeneities to develop.

The degree of clusterization can be conveniently characterized by the inhomogeneity factor:  $r = \langle n \rangle / n_0$  where  $n_0$  is the initial density and

$$\langle n(t) \rangle = \frac{1}{n_0 L^3} \int f(\vec{r}, \vec{p}; t) n(\vec{r}; t) d\vec{r} d\vec{p} \quad (7)$$

This factor remains equal to 1 for homogeneous systems and grows as soon as clusters develop. Time evolutions of this factor are shown in figure 3 for a cold ( $T=0$ ), dilute system ( $n_0$  is less than  $1/3$  of the normal nuclear matter) initial system, with several Skyrme interactions. In all our calculations, such curves exhibit a typical S-shape when the spinodal decomposition occurs: three regimes are present: an initial regime where  $r$ -factor rises slowly, it corresponds to the progressive building up of the fluctuations; the fragmentation regime where the initial stable state is destroyed by the fluctuations and clusters are formed as shown by the rapid upsurge of the  $r$ -factor; finally an asymptotic regime where  $r$ -factor keeps its limit value which depends on the initial preparation of system.

The fragmentation regime corresponds to the rapid amplification of the initial fluctuations present in the system which intervene as 'seeds' of the process. In our simulation most initial fluctuations are purely numerical, mainly from uncomplete sampling of the phase space.

In figure 4, we show the behaviour of the system when modifying the initial sampling of the phase space : less pseudo-particles means more initial fluctuations. One sees that the first regime is shorter, the system needs less time to build up the fluctuations, but the second regime is quite similar, which means that the system loses memory of its initial preparation as expected in chaotic transitions. Then, the duration of the first regime of the S-shape curve is meaningless since 'sampling-dependent' : in particular it depends on the random generator seeds. We shall determine the time characteristic of the fragmentation as the non-ambiguous time duration of the second regime, namely the  $t_{10-90}$  time of the density evolution.

$$t_{10-90} = t(\langle n \rangle = 0.9 \langle n \rangle_\infty) - t(\langle n \rangle = 0.1 \langle n \rangle_\infty) \quad (8)$$

where  $\langle n \rangle_\infty$  is the asymptotic value of  $\langle n \rangle$ .

In figure 3, one sees that multifragmentation clearly depends on the interaction. The small difference between the asymptotic densities being connected with the differences in the excitation energies of the system. All these interactions give more or less the same saturation properties for nuclear matter. Nevertheless they have important differences for quantities like incompressibility  $K_\infty$  and effective mass  $m^*/m$ . Such parameters are expected to have an important role in the evolution of  $\langle n \rangle$  in time; surface parameters like the surface energy coefficient  $a_s$  have also to be considered because surface phenomena are important in cluster formation. We were able to fit all the  $t_{10-90}(n, T)$  (within a 15% relative error) using an empirical formula as the following.

$$t_{10-90}(n, T) = A [-K(n, T)]^a \left[ \frac{m^*(n)}{m} \right]^b \left[ \frac{a_s(n_0)}{T_c - T} \right]^c \left[ 1 - \left( \frac{n - n_c}{n_0} \right) \right]^d \quad (9)$$

for  $(n, T)$  inside the spinodal zone.

$K(n, T)$  is the isotherm incompressibility,  $(n_c, T_c)$  the critical density and temperature and  $n_0$  the saturation density of nuclear matter at  $T=0$ . The  $t_{10-90}$  is directly given in  $\text{fm/c}$  with the following set of parameters :  $A = 20450 \text{ MeV}^{1.12} \cdot \text{fm/c}$ ,  $a = -1.12$ ,  $b = 0.5$ ,  $c = 0.7$  and  $d = 0.1$ .

In our investigations, typical values for  $t_{10-90}$  are in between 60 fm/c and 200 fm/c depending on the initial value  $(n,T)$ . This can be seen in particular for  $Skm^*$  in figures 5a and 5b.

In figures 5a and 5b, we evidence the spinodal zone by variations of the initial preparation in the  $(T,n)$  plane. Firstly, we notice that when prepared inside the spinodal zone the inhomogeneities do grow, and when prepared outside ( $n=0.11 \text{ fm}^{-3}$ ) the system remains homogeneous. This illustrates the ability of the model to accurately simulate the genuine Nuclear Equation Of State. Secondly, the characteristic time for multifragmentation (i.e. the  $t_{10-90}$  parameter) is strongly dependent of  $n(t=0)$  (figure 5a) and  $T(t=0)$  (figure 5b). Closer to the critical temperatures ( $T=12 \text{ MeV}$ ) the superficial tension almost vanishes and densities homogeneities grow very slowly. The more dilute and the cooler the system the faster the process, since the spinodal decomposition leads to the formation of relatively cold drops inside a dilute gas.

Figure 6 shows that the Uehling-Uhlenbeck collision term increases by 15% the asymptotic  $r$ -factor. The  $t_{10-90}$  does not significantly change due to the low density of the system while fluctuations building up and early clusters formation.

In conclusion, we have been able to characterize the clusterization time,  $t_{10-90}$ , in nuclear matter in a way which is independent of the sampling of the phase space. It was shown that  $t_{10-90}$  is strongly dependent on the coordinates  $(n,T)$  of the initial condition in the spinodal zone and on the nuclear interaction itself. Clusterization times are ranging between 60 fm/c to 200 fm/c. A realistic interaction like  $Skm^*$  gives  $t_{10-90}$  around 100 fm/c in the most favourable case of cold and dilute nuclear matter. During heavy-ion collisions the compound system could undergo such a decomposition if it spends time enough in the spinodal zone. From the previous results such a phenomena could be tracked in the core of two large nuclei colliding at low energy around 30 MeV/u.

The authors are grateful to Pr. D.H. Boal for interesting e-mail exchanges.

## References

- [1] C.J. Pethick and D.G. Ravenhall, *Ann. Phys. (N.Y.)* 183, 131 (1988).
- [2] H. Heiselberg, C.J. Pethick and D.G. Ravenhall, *Phys. Rev. Lett.* 61, 818 (1988).
- [3] G. Peilert, J. Randrup, H. Stöcker and W. Greiner, *Phys. Lett. B* 260,271 (1991).
- [4] D.H. Boal and J.N. Glosli, *Phys. Rev. C* 42, 502 (1990).
- [5] S. Das Gupta and G.F. Bertsch, *Phys. Rep.* 160, 189 (1988).
- [6] C. Grégoire, B. Remaud, F. Sebillé, L. Vinet and Y. Raffray, *Nucl. Phys. A*465, 77 (1987).
- [7] D. Idier, M. Farine, B. Remaud and F. Sebillé, LPN report (1992) to be published.
- [8] J. Bartel, P. Quentin, M. Brack, C. Guet and H.B. Hakansson, *Nucl. Phys. A*386, 79 (1982).
- [9] M. Beiner, H. Flocard, N. V. Giai and P. Quentin, *Nucl. Phys. A*238, 29 (1975).
- [10] F. Tondeur, M. Brack, M. Farine and J.M. Pearson, *Nucl. Phys. A*420, 297 (1984).
- [11] F. Tondeur, *Nucl. Phys. A*315, 353 (1987).

## Figure captions

Figure 1 : Comparison between Hartree-Fock calculations and Pseudo-Particle Model : total energy per nucleon ( $E/A$ ) versus density ( $n$ ) at  $T=0, 5, 10$  MeV, for Skyrme Skm\* force.

Figure 2 : Snapshots of the positions of pseudo-particles at  $t=0$  and  $t=165$  fm/c. The nine cells evidence the cyclic boundary conditions.

Figure 3 : Dynamical computation of convoluted density  $\langle n \rangle$  for several Skyrme type forces SIII and SVI [9], T1 and T5 [10], To78 [11], Zam 228 and Zam 300 mean simplified ( $t_0, t_3$ ) Skyrme interactions with  $K_{\infty}=228$  MeV and  $K_{\infty}=300$  MeV. The starting density is  $0.0492 \text{ fm}^{-3}$  (i.e.  $k_F=0.9 \text{ fm}^{-1}$ ) and initial temperature  $T=0$ .

Figure 4 : Effect of the number of pseudo-particles per nucleon  $n_g$  on the time-evolution of convoluted density  $\langle n \rangle$ . Below  $n_g=20$ , calculations are not relevant.

Figure 5a : Skm\* spinodal zone. Time-evolution of the convoluted density  $\langle n \rangle$  at several initial temperatures :  $T=0, 3, 6, 9$  and  $12$  MeV. Starting density is  $0.0492 \text{ fm}^{-3}$ .

Figure 5b : Time-evolution of the convoluted density  $\langle n \rangle$  at  $T=3$  MeV, for several initial densities:  $n=0.02, 0.0492, 0.08$  and  $0.11 \text{ fm}^{-3}$ . Last point ( $0.11 \text{ fm}^{-3}$ ) is outside of the Skm\* spinodal zone.

Figure 6 : Effect of the Uehling-Uhlenbeck collision term (here  $n_g=31$ ).

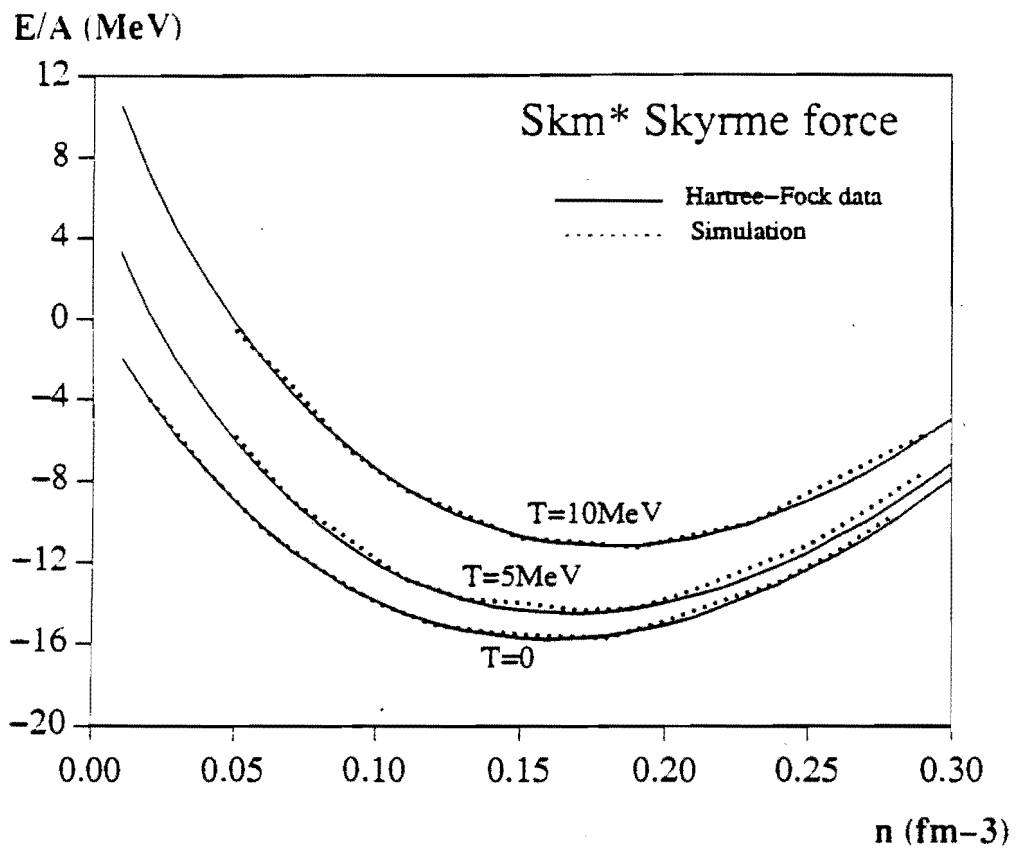
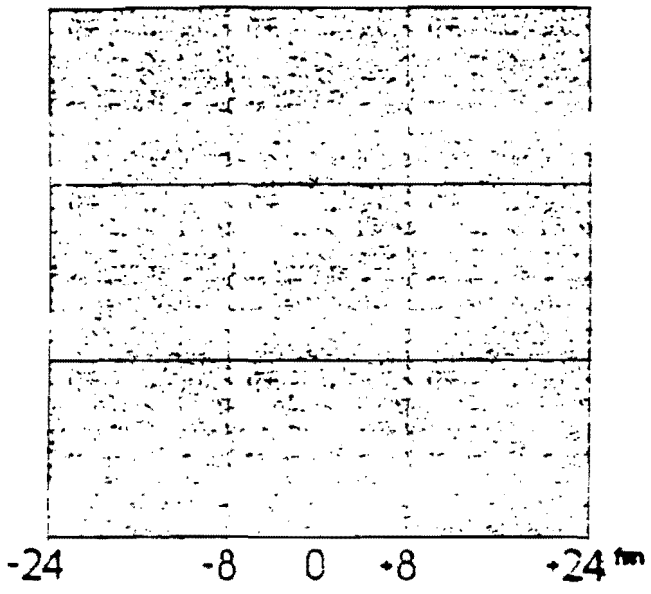
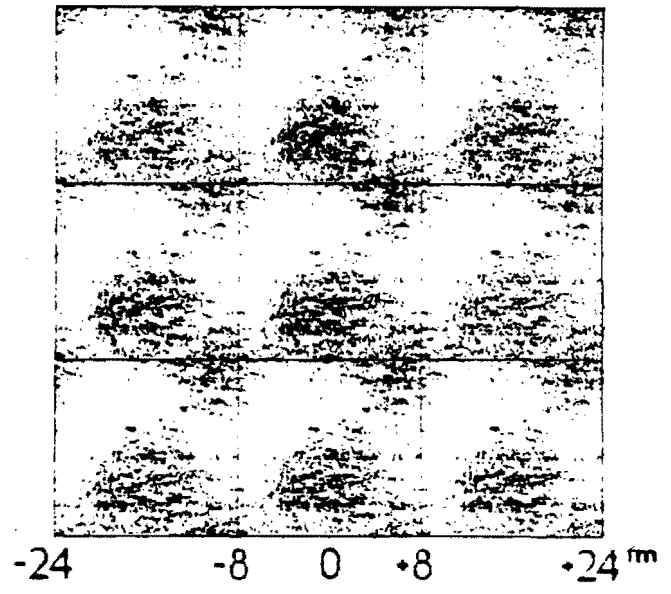


Figure 1



$t = 0$



$t = 165 \text{ fm}/c$

Figure 2

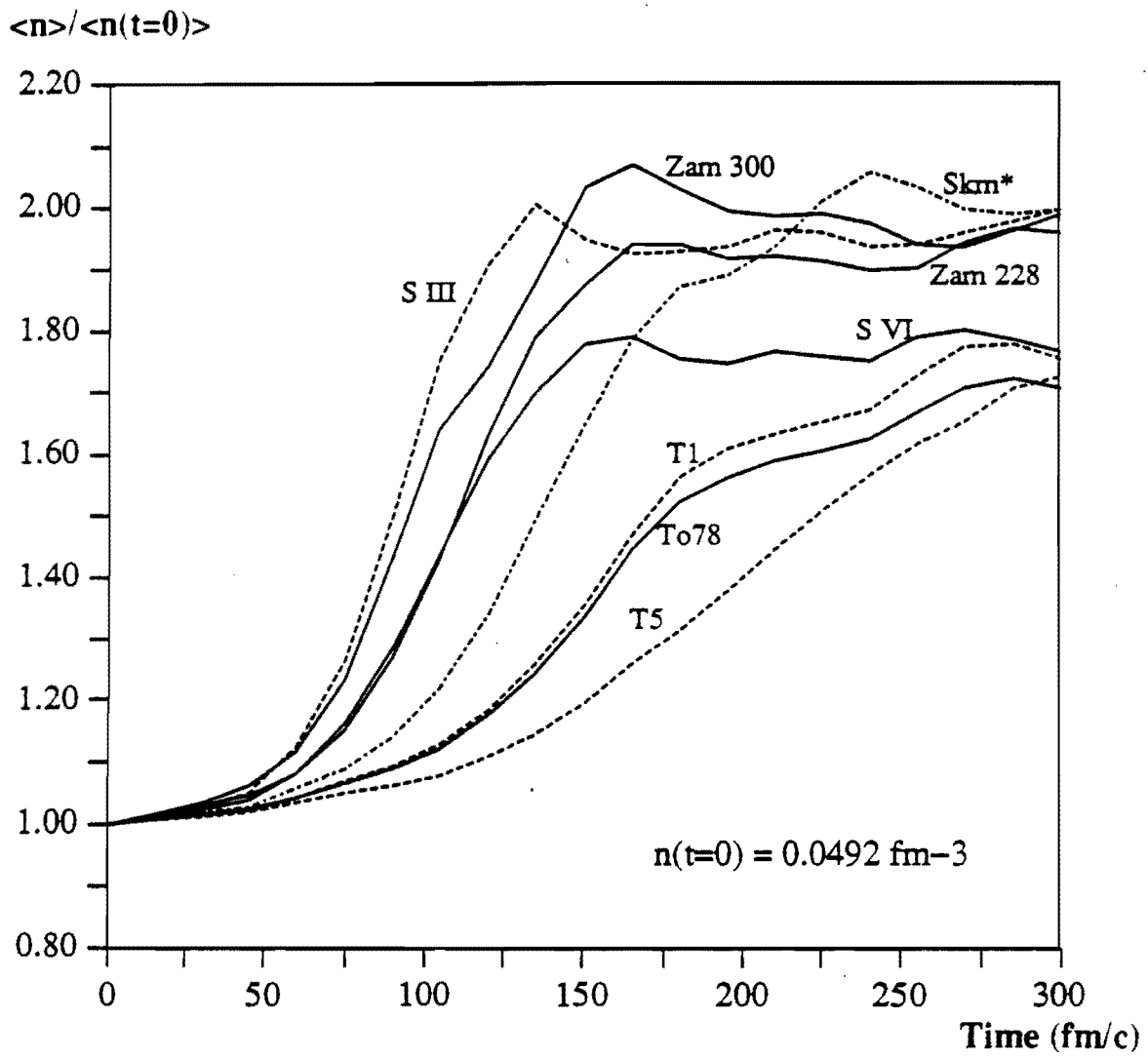


Figure 3

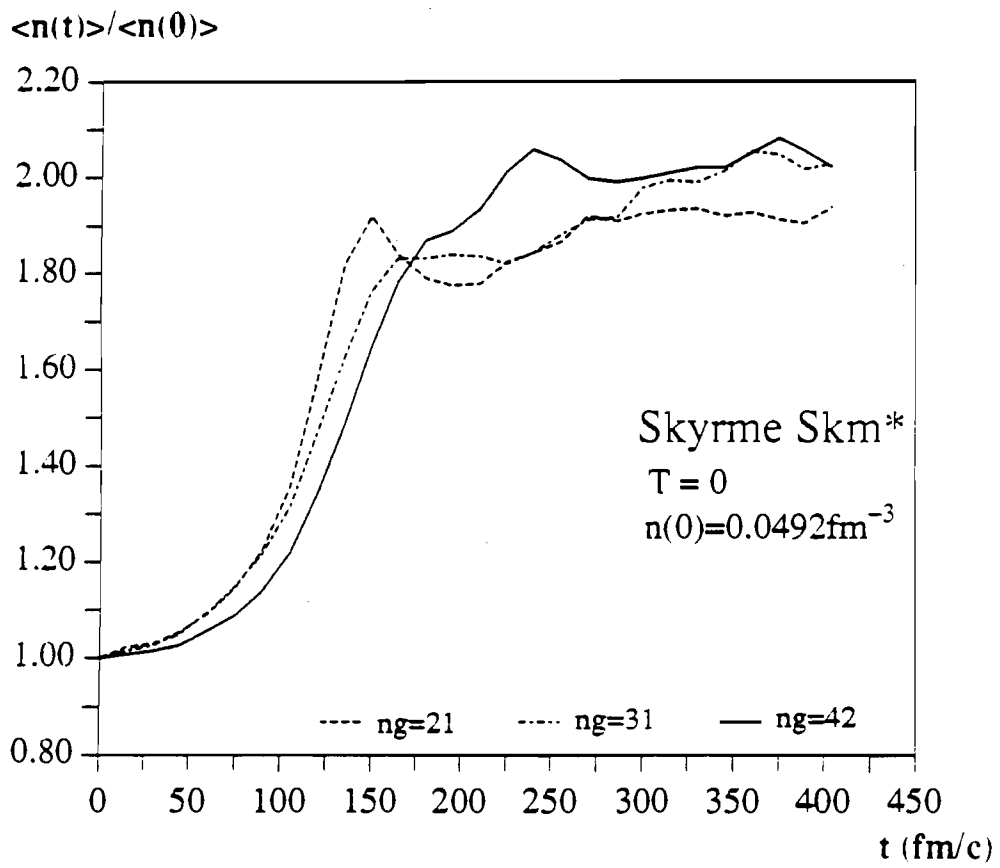


Figure 4

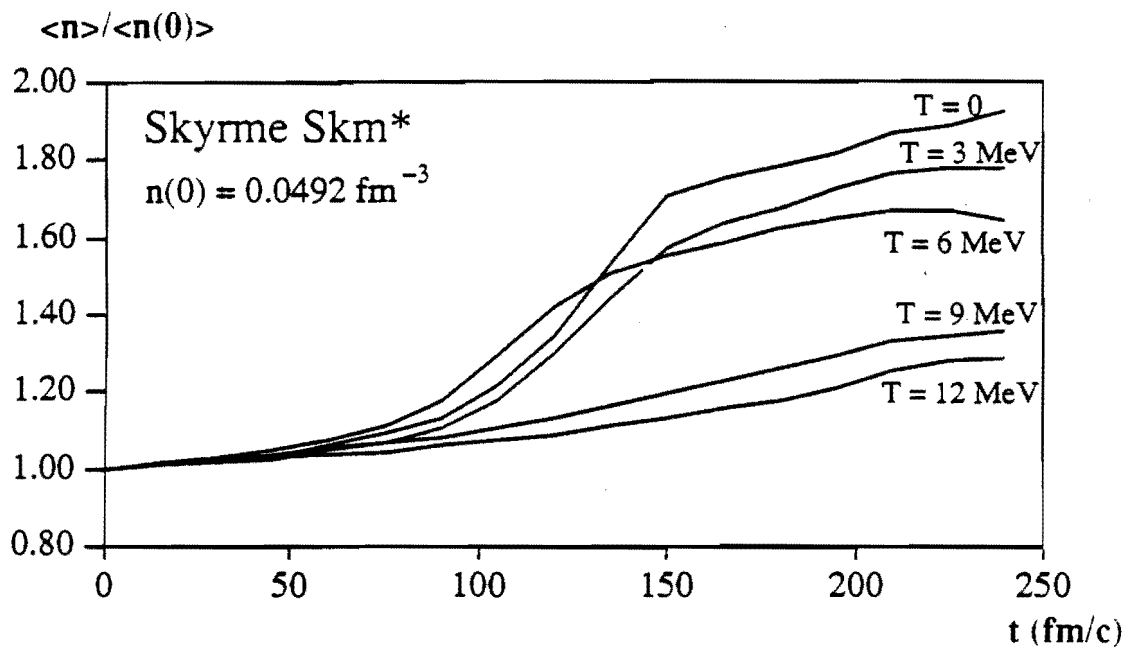


Figure 5a

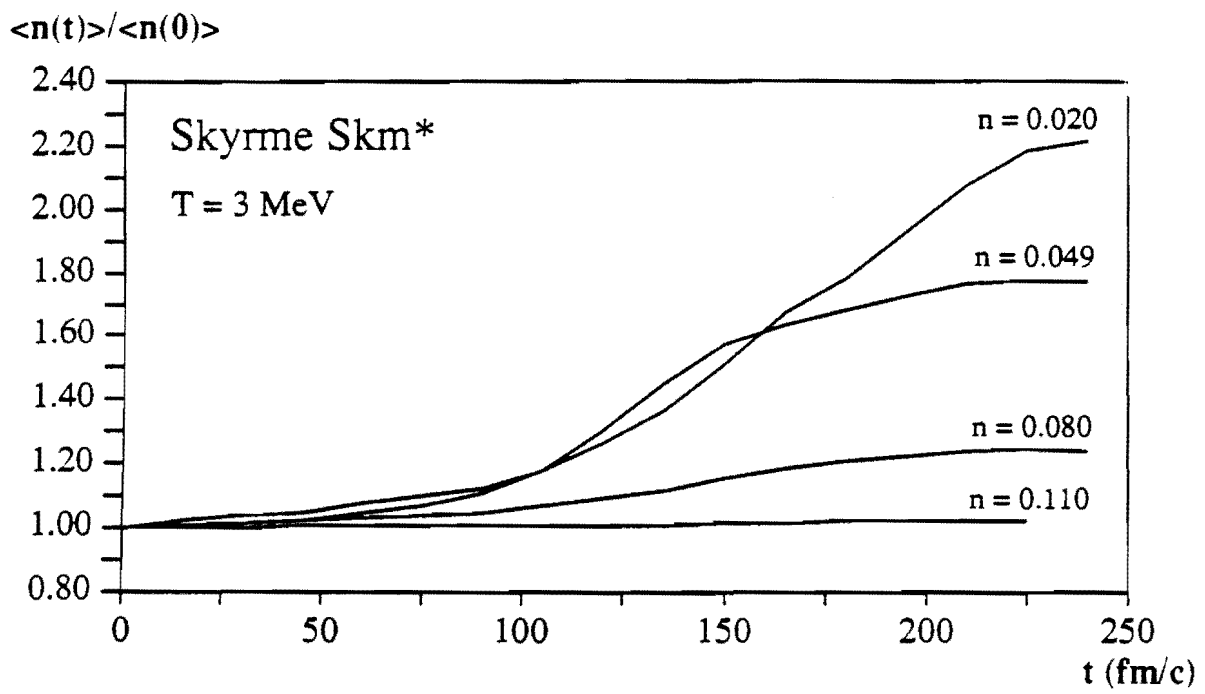


Figure 5b

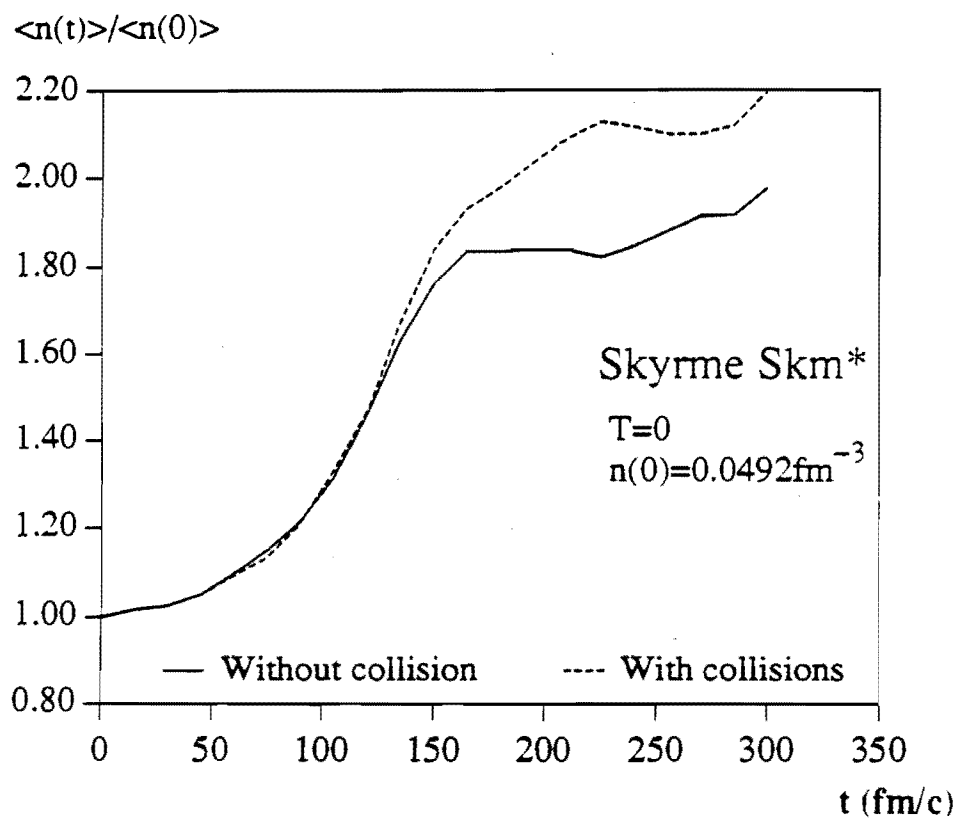


Figure 6